Synthesis and photovoltaic properties of novel solution-processable triphenylamine-based dendrimers with sulfonyldibenzene cores†

Kunpeng Li, Jiali Qu, Bin Xu, Yinhua Zhou, Leijing Liu, Ping Peng and Wenjing Tian*

Received (in Montpellier, France) 5th June 2009, Accepted 15th July 2009
First published as an Advance Article on the web 10th August 2009
DOI: 10.1039/b9nj00236g

Three conjugated dendrimers containing electron-accepting sulfonyldibenzene (SDB) cores and electron-donating triphenylamine dendrons have been synthesized through a convergent synthetic strategy without any protection/deprotection chemistry. The dendrimers were highly soluble in common organic solvents, and could form good quality optical films by spin coating. Their thermal, optical and electrical properties are manipulated by attaching different peripheral dendrons. Using these dendrimers as donors and [6,6]-phenyl C61-butyric acid methyl ester (PCBM) as acceptor, the bulk heterojunction solar cells with a structure of ITO–PEDOT–dendrimers:PCBM–LiF–Al were fabricated. The cell based on dendrimer **G0** shows a relatively high power-conversion efficiency (PCE) of 0.34% under AM 1.5 illumination of 100 mW cm^{-2}.

Introduction

In the past decade, organic solar cells (OSCs) have been extensively investigated because of their advantages of low-cost, light weight, and easy fabrication.[1–7] Since the 1%-efficient thin-film OSCs based on a single donor–acceptor (D–A) heterojunction was reported by Tang,[8] the power-conversion efficiency (PCE) of OSCs has steadily improved through the design and synthesis of new materials and the optimization of the cell structures. Among the new active materials, small-molecules have advantages such as well-defined molecule structure, relatively simple and reproducible synthesis and purification, its monodisperse nature, ability to be vacuum deposited in multi-layer stacks, and so on. For the purpose of practical applications, nevertheless, small molecules have to be processed by expensive techniques, for example, vacuum sublimation and vapor deposition, which are not well suited to the manufacture of large size devices. Polymers are generally of lower purity than small molecules but can achieve larger size films at much lower costs using solution-based deposition techniques such as spin coating, inkjet, and roll-to-roll printing. Thus, the ideal materials should have advantages of both small molecules and polymers.

Dendrimers with molecular weights in the favorable range between 1000–10 000 g mol^{-1} can be purified to a high degree using chromatographic techniques, and deposited into a thin film from solution by a simple spin-coating process.[9]

Meanwhile, triphenylamine (TPA) derivatives have shown excellent thermal and electrochemical stability, electron donating ability, and isotropic optical and charge-transport properties as well as a three-dimensional propeller structure.[10,11]

On the other hand, molecules with D–π–A structure have many advantages, such as lower bandgap due to the intramolecular charge transfer (ICT) between the donor and acceptor and easily controlled energy levels by introducing acceptor and donor moieties with different pull–push electron abilities into the molecules.[12] So considerable research efforts have led to much progress in the synthesis of new molecules which mainly consist of a TPA moiety linked to different acceptor moieties, including dicyanovinyl, perylene, benzothiadiazole, or 2-pyran-4-ylidenemalononitrile.[13,14]

Therefore, dendrimers containing triphenylamine dendrons and the D–π–A structure could be expected to be one of the ideal active molecules for the application of thin-film OSCs.

In this paper, we designed and synthesized three novel dendrimers with symmetrical donor–π-bridge–acceptor–π-bridge–donor (D–π–A–π–D) structure with sulfonyldibenzene as the core and triphenylamines as dendrons. These conjugated dendrimers have good solubility in common organic solvents, such as chloroform, dichloromethane, 1,2-dichloroethane, and THF *etc*. They also exhibit good film forming properties which is of great importance for their application in photovoltaic devices. We investigated the photovoltaic properties of the three dendrimers by fabricating the bulk heterojunction solar cells with a structure of ITO–PEDOT–dendrimers:PCBM–LiF–Al, and the PCEs of the solar cells based on the three dendrimers are 0.34%, 0.19% and 0.06%, respectively.

Results and discussion

Synthesis of materials

The synthetic routes to the core and dendrons as well as the dendrimer are shown in Scheme 1 and Scheme 2. Compound **1**

State Key Laboratory of Supramolecular Structure and Materials, Jilin University, Changchun 130012, China.
E-mail: wjtian@jlu.edu.cn; Fax: +86 431 85193421; Tel: +86 431 85166368

† Electronic supplementary information (ESI) available: Supplementary figures, tables and spectra. See DOI: 10.1039/b9nj00236g

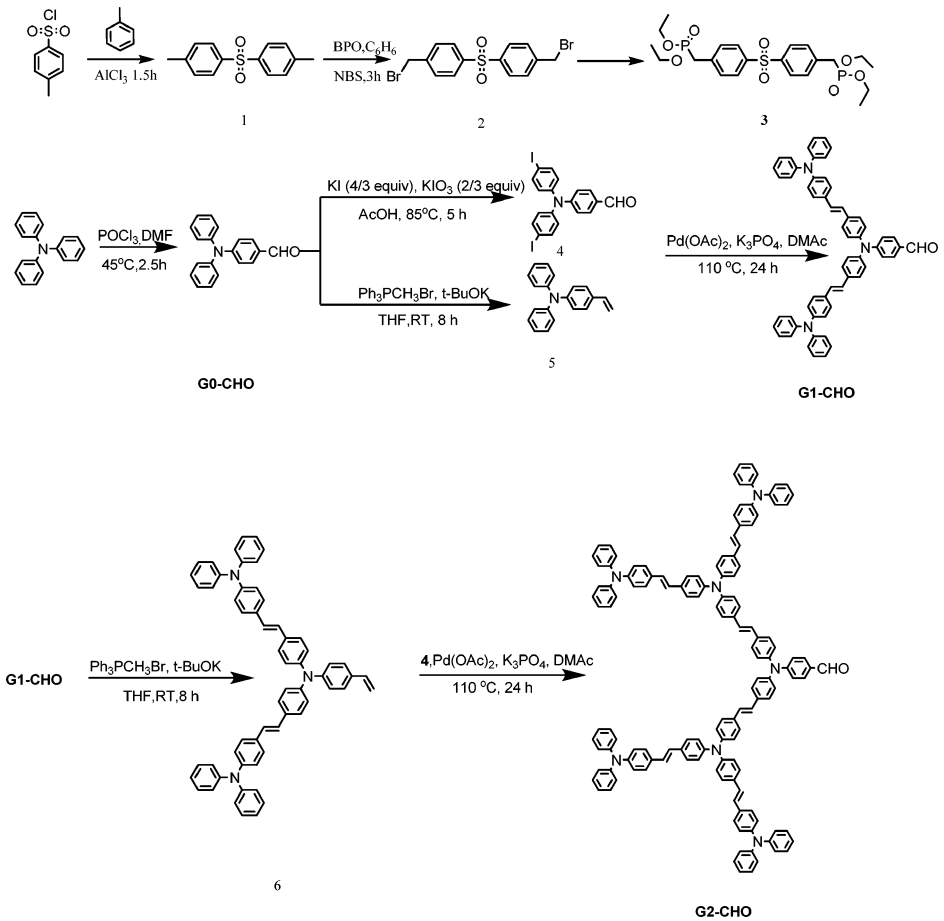

Scheme 1 Synthesis of the sulfonyldibenzene core and TPA-based dendrons.

was synthesized by a Friedel–Crafts acylation from 4-methylbenzene-1-sulfonyl chloride and toluene with a yield of 68%. The bromination of compound **1** by employing *N*-bromosuccinimide (NBS) in benzene successfully afforded the desired compound **2**. Compound **3** can be easily prepared from compound **2** through the reaction with the triethyl phosphate under the protection of N_2. The strategy as reported by our group[15] for the synthesis of the aldehyde-focused dendron is illustrated in Scheme 1. Firstly, 4-(diphenylamino)-benzaldehyde, which is the first generation aldehyde-focused dendron **G0–CHO**,[16,17] was readily obtained from TPA through a Vilsmeier reaction in a yield of 90%. Then, iodination of **G0–CHO** with KI–KIO_3 in AcOH at 85 °C provided compound **4**[18] with a good yield of 95%, and the compound **5** was prepared in a 76% yield from the reaction of **G0–CHO** with methyltriphenylphosphonium bromide. After that, the second generation aldehyde-focused dendron **G1–CHO** was prepared in a 55% yield *via* the coupling of compound **4** and compound **5** through the Heck reaction.[19] The third generation aldehyde-focused dendron **G2–CHO** can be obtained from compound **4** and compound **6** through the Heck reaction, while compound **6** can be synthesized by the Wittig reaction[20] of **G1–CHO** and methyltriphenylphosphonium bromide. The first-generation of dendrimer **G0** was synthesized *via* a typical Wittig–Horner reaction between aldehyde **G0-CHO** and compound **3** in dry THF, using potassium *tert*-butoxide as base in a yield of 78%. The second and third generation **G1** and **G2** were obtained through the same synthetic method in yields of 61% and 45%, respectively. Dendrons and dendrimers were characterized by ^{1}H NMR, ^{13}C NMR, FT-IR, elemental analysis and MALDI-TOF mass spectroscopy. **G0**, **G1** and **G2** exhibit an IR absorption band around 960 cm^{-1} arising from the wagging vibration of the *trans*-double bond.[21,22] Additional definitive evidence for the molecular structures of the dendrimers was obtained from MALDI-TOF mass spectra. And the deviation between the calculated and experimentally measured m/z values was no more than one mass unit.

Thermal properties

The differential scanning calorimetry (DSC) second heating thermograms of **G0**, **G1** and **G2** recorded at a scanning rate of 10 °C min^{-1} under nitrogen protection indicated that the Tg of **G0**, **G1** and **G2** (81 °C, 138 °C and 175 °C) increases gradually, due to the reduced segmental motions and enhanced intermolecular dipolar interaction to a certain extent (see Fig. S1, ESI†).

Absorption

Fig. 1 shows the UV-vis absorption spectra of the dendrimers in films coated on quartz substrate. **G0** displays two

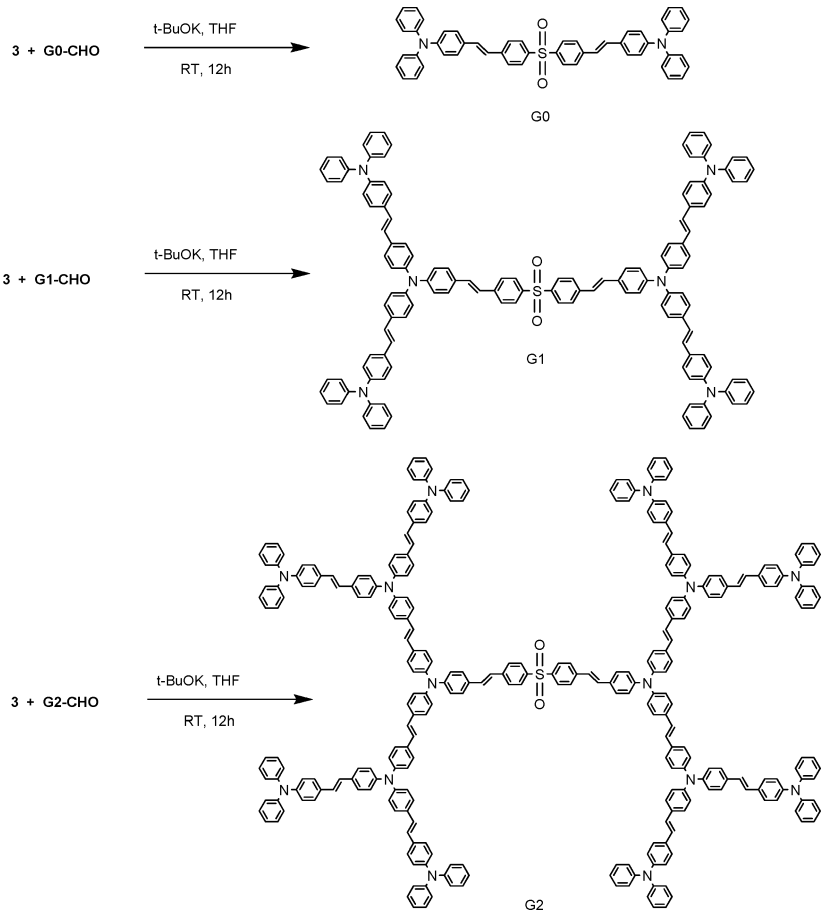

Scheme 2 Synthesis of the sulfonyldibenzene-based dendrimers.

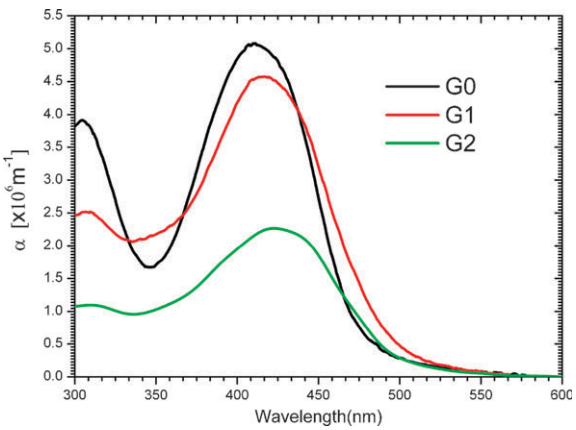

Fig. 1 UV-vis absorption-coefficient (α) spectra of **G0**, **G1** and **G2** in the films. All films were measured on a glass–ITO–PEDOT:PSS substrate and corrected for substrate absorption.

absorption peaks at 304 nm and 410 nm, which are ascribed to the absorption of the n–π* transition of the SDB moiety and the intramolecular charge transfer between the TPA donor and the SDB acceptor, respectively. It was also observed that **G1** displayed two absorption peaks at 307 nm and 416 nm, and **G2** at 311 nm and 419 nm. Comparing with **G0**, the ICT transitions of **G1** and **G2** red-shift 6 nm and 9 nm, respectively. This explains that the increase of TPA units with the increasing generations of dendrimers results in the extension of the conjugated length and a stronger electron-donating ability of the donor parts in **G1** and **G2**. It also indicates that the conjugated length in the dendrimers could be increased by the introduction of TPA units,[23] but the increasing degree might be saturated when the conjugated chain was enlarged to a certain extent by such large size and non-coplanar TPA dendrons.

It is noted that the *Y*-axis in Fig. 1 represents the extinction coefficient (α) of the three dendrimer films with the same thickness. The decrease of the extinction coefficient from **G0** to **G2** films is due to the large size of TPA dendrons which occupy a large space in the dendrimer films. When the thickness of the films of **G0**, **G1** and **G2** is the same (70 nm), the molecule number of **G2** in the film is less than those of **G0** and **G1**, resulting in less ICT transition and ultimately the decrease of the absorption from **G0** to **G2** films. The UV and PL spectra of **G0**, **G1** and **G2** in solution can be seen in the ESI.†

Electrochemistry

Fig. 2 shows the cyclic voltammetry (CV) diagrams of the three dendrimers in CH_2Cl_2 in the presence of $TBAPF_6$ as the supporting electrolyte with platinum button working electrodes, a platinum wire counter electrode and an $Ag/AgNO_3$ reference

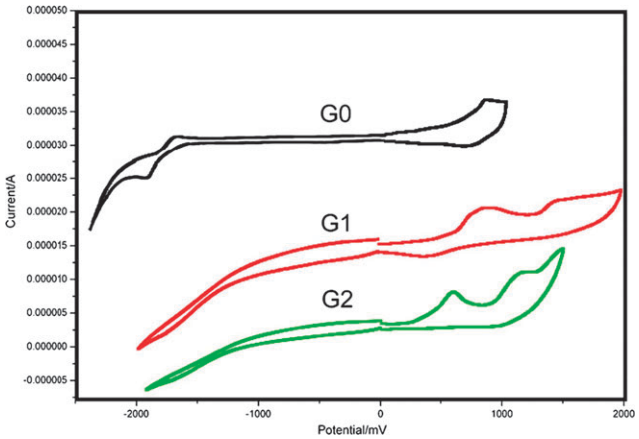

Fig. 2 CV diagrams of the three dendrimers in CH_2Cl_2.

electrode under an N_2 atmosphere. The redox potential of Fc/Fc^+, which has an absolute energy level of −4.8 eV relative to the vacuum level for calibration, is located at 0.20 V in $TBAPF_6$ (0.1 M)–CH_2Cl_2 solution at a scan rate of 100 mV S^{-1}. The CV curve of **G0** shows a pair of reversible redox peaks in the negative region because of the high electrical activity of the SDB core, but there are no redox peaks in the negative region for **G1** and **G2** due to the surrounding effect of TPA flock. In the positive region, the oxidation peaks of **G0**, **G1** and **G2** can be attributed to TPA donating groups. The onset oxidation potentials (E_{Ox}^{onset}) are observed at +0.67 V, +0.63 to +0.45 V for **G0**, **G1** and **G2**. The evaluation of the highest occupied molecular orbital (HOMO) and the lowest unoccupied molecular orbital (LUMO) energy levels can be done according to the following equations:[24]

$$\text{HOMO (eV)} = -(eE_{Ox}^{onset} + 4.60\ \text{eV}) \quad (1)$$

$$\text{LUMO (eV)} = -(eE_{Red}^{onset} + 4.60\ \text{eV}) \quad (2)$$

where E_{Ox}^{onset} and E_{Red}^{onset} are the onset redox potentials relative to Ag/Ag^+.[25] The electrochemical properties as well as the energy levels of **G0**, **G1** and **G2** are summarized in Table 1.

The HOMO energy levels of **G0**, **G1** and **G2** is −5.27 eV, −5.23 eV and −5.05 eV, respectively, which means that with the increase of the number of TPAs in the external group, the electron-donating ability of the external groupis enhanced. The LUMO energy level of **G0** is obtained from eqn (2), while those of **G1** and **G2** were estimated from the HOMO energy level and the optical band gap (Eg^{opt}).[26] The LUMO energy levels of the three dendrimers are similar due to their containing the same acceptor group SDB.

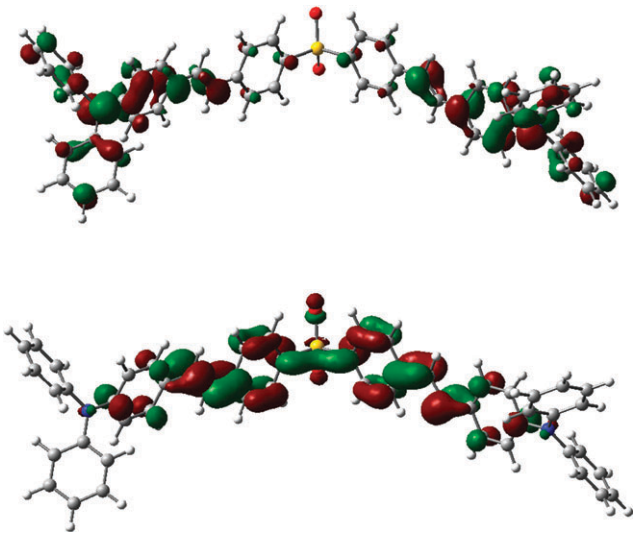

Fig. 3 The HOMO (top) and LUMO (bottom) orbitals in the optimized ground-state structure of **G0**.

Quantum-chemical calculations

In order to investigate the electron distribution of the LUMO and HOMO energy levels of the dendrimers, quantum-chemical calculations were carried out through the Gaussian 03 program at the B3LYP/6-31G* level.[27] Fig. 3 shows the electron distribution of the LUMO and HOMO in the optimized ground-state structure of **G0**. Comparison of the electron distribution in the frontier on the molecular orbitals reveals that the HOMO is localized on the triphenylamine donor moiety, while the LUMO is localized on the sulfonyl-dibenzene acceptor moiety, which is generally an indication of a HOMO → LUMO absorption transition bearing a significant charge-transfer character.[28,29]

Photovoltaic properties

In order to investigate the photovoltaic properties of the three dendrimers, bulk heterojunction solar cells (cell 1, cell 2 and cell 3) with **G0**, **G1** and **G2** as donors and PCBM as an acceptor were fabricated. Devices based on compound–PCBM blend films with varied ratios (2 : 1, 1 : 1, 1 : 2, 1 : 3, 1 : 4) were prepared, and the active layer thickness was optimized. We found that when the blend ratio reaches 1 : 2, the device performance is the best and 65–70 nm is the best active layer thickness for all kinds of devices. Detailed information is listed in Table S1 ESI.† The monochromatic incident photon-to-electron conversion efficiency (IPCE) spectra of the three cells under monochromatic irradiation are shown in Fig. 4, which coincide well with the absorption spectra of the three active

Table 1 The electrochemical properties and energy levels of **G0**, **G1** and **G2**

Dendrimer	E_{Ox}^{onset}/V	E_{Red}^{onset}/V	HOMO/eV	LUMO/eV	Eg^{opt}[a]/eV	Eg^{el}[c]/V
G0	0.67	−1.8	−5.27	−2.8	2.59	2.47
G1	0.63	—	−5.23	−2.78[b]	2.45	—
G2	0.45	—	−5.05	−2.75[b]	2.30	—

[a] The Eg^{opt} was obtained from the absorption edge. [b] LUMO of **G1** and **G2** is calculated by the equation |LUMO| = |HOMO| − Eg^{opt}. [c] Eg^{el} = band gap from electrochemistry.

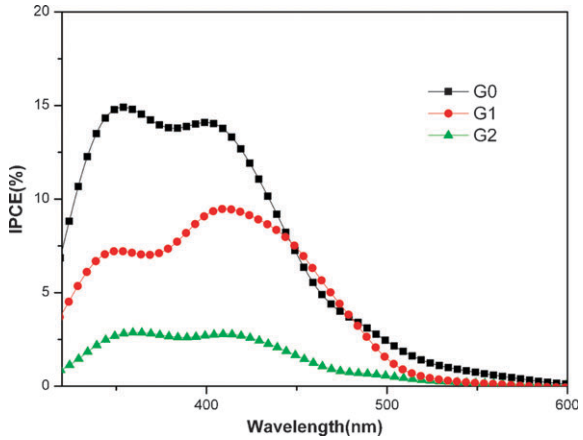

Fig. 4 Photocurrent action spectra of bulk heterojunctions of **G0–2** and PCBM (1 : 2, w/w) under monochromatic irradiation.

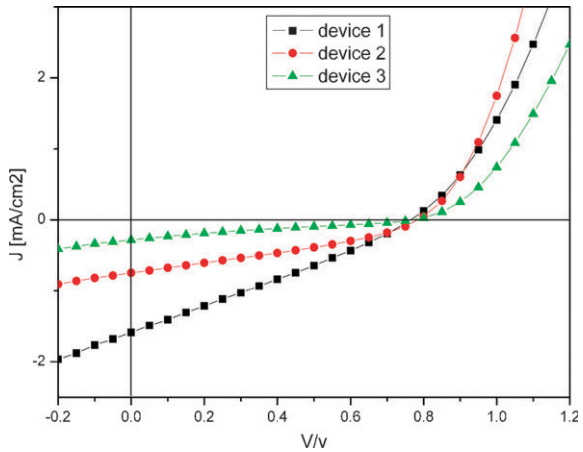

Fig. 5 Current–voltage curves of cells prepared from the active layers of dendrimers : PCBM (1 : 2, w/w) under AM 1.5 G irradiation with an intensity of 100 mW cm^{-2}.

layers. The photoresponse in the range of 300–360 nm is from the absorption of n–π* and PCBM and that in the visible region 370–550 nm is mainly from the absorption of ICT from the donor to the acceptor. The different IPCEs of the three cells originated from the different PCEs.

Fig. 5 shows the current density–voltage (*I–V*) characteristics of the solar cells with the thickness of an active layer of 70 nm under AM 1.5 (AM: air mass) illumination with an intensity of 100 mW cm^{-2}. Cell 1 has the best PCE of 0.34% compared with cell 2 and cell 3, with a relatively high short circuit current (I_{sc}) of 1.6 mA cm^{-2}, an open circuit voltage (V_{oc}) of 0.79 V and a fill factor (FF) of 0.28, which is relatively lower than the PCE of solar cells based on donor–acceptor molecules reported in other papers.[14,30] Cell 2 reveals I_{sc} of 0.74 mA cm^{-2}, so despite the equal V_{oc} and higher FF (0.32), the PCE is about half of that of cell 1. For cell 3, the V_{oc} decreases slightly to 0.77, with an FF equal to 0.28, and a PCE of 0.06%. The photovoltaic parameters of the solar cells are summarized in Table 2. It can be seen that the drop of PCE from **G0** to **G2** mainly results from the drop of I_{sc}. As we know, I_{sc} is firstly determined by the absorption of the active layer. Comparing the absorptions of **G0**, **G1** and **G2** in Fig. 1, **G1** and **G2** absorb larger-wavelength photons, which is beneficial to I_{sc}. But the extinction coefficients of **G1** and **G2** are lower than that of **G0**, which means **G0** absorbs more photons than **G1** and **G2** in a film with the same thickness. Meanwhile, the low I_{sc} of **G2** is caused by the aggregated configuration in a **G2**–PCBM blend film. The AFM images of blend films of **G0**–PCBM and **G2**–PCBM, as shown in Fig. S2 (ESI†), reveal a roughness with root mean square (RMS) 0.45 nm and 2.23 nm, respectively, which reveals that **G0** has better film-forming properties compared with **G2**. The poor solubility due to the huge molecular weight of **G2** may lead to the bad film-forming ability. The better photovoltaic behavior obtained with **G0** as a donor should be ascribed to the synergistic effects of its enhanced absorption of incident light, high quality uniform spin-cast film.

Table 2 Summary of cell performance for ITO–PEDOT–dendrimers: PCBM–LiF–Al based solar cells

	Dendrimer : PCBM (w/w ratio)	V_{oc}/V	I_{sc}/mA cm^{-2}	FF	η (%)
G0	1 : 2	0.79	1.6	0.28	0.34
G1	1 : 2	0.79	0.74	0.32	0.19
G2	1 : 2	0.77	0.28	0.28	0.06

Conclusion

In conclusion, we have synthesized three conjugated dendrimers bearing electron-accepting sulfonyldibenzene groups as the cores, and TPA moieties as electron-donating dendrons, through a convergent synthetic strategy without any protection/deprotection chemistry. The dendrimers are highly soluble in common organic solvents, and could form excellent-quality optical films by spin coating. Their thermal, optical and electrical properties are manipulated by attaching different peripheral dendrons. Quantum-chemical calculations of electronic structure show that the HOMO and LUMO of **G0** are highly localized on the donor and acceptor moieties, respectively. Using **G0**, **G1** and **G2** as donors and PCBM as an acceptor, bulk heterojunction solar cells with a structure of ITO–PEDOT–dendrimers:PCBM–LiF–Al were fabricated. The cell based on **G0** shows a relatively high PCE of 0.34%.

Experimental

General

All chemicals, reagents, and solvents were used as received from commercial sources without further purification. Tetrahydrofuran (THF) was refluxed with sodium and benzophenone, and distilled. ^{1}H NMR and ^{13}C NMR spectra were recorded on an AVANCE 500 spectrometer and a Varian Mercury-300 NMR, with tetramethylsilane (TMS) as the standard. The FT-IR spectra were recorded *via* the KBr pellet method by using a Nicolet Impact 410 FT-IR spectrophotometer. The mass spectra were recorded on a Kratos MALDI-TOF mass spectrometer, and the spectra were recorded in the reflection mode with anthracene-1,8,9-triol as the matrix. The synthetic routes to the core and dendrons as well as the dendrimer are shown in Scheme 1 and Scheme 2.

Dendrons and dendrimers were characterized by ^{1}H NMR, ^{13}C NMR, FT-IR, elemental analysis and MALDI-TOF mass spectroscopies. UV-vis absorption spectra were measured using a Shimadzu UV-3100 spectrophotometer. Film thickness was recorded on a Veeco Dektak 150 Surface Profiler. AFM images were obtained using a Nanoscope IIIa Dimension 3100. The OSCs were fabricated in the configuration of the traditional sandwich structure with an indium tin oxide (ITO) anode and metal cathode. A thin layer of poly(3,4-ethylenedioxythiophene)–poly(styrene sulfonate) (PEDOT:PSS) (Baytron, PVP 4083, Germany) was spin-coated onto the ITO glass and dried in a vacuum oven at 120 °C for 20 min. Subsequently, the active layer was prepared by spin coating the composite chloroform solution of dendrimer : PCBM (1 : 2, w/w) on the top of the PEDOT:PSS layer. The cathode, a bilayer of a thin (1 nm) LiF layer covered with 100 nm Al, was thermally evaporated through a mask at a pressure of 5×10^{-4} Pa. The active area of the cell was 5 mm^2. Cell characterization was performed under AM 1.5 G irradiation with an intensity of 100 mW cm^{-2} on an Oriel Xenon solar simulator. Current–voltage characteristics were recorded with a Keithley 2400.

Synthesis

Compound 1. A mixture of 4-methylbenzene-1-sulfonyl chloride (7.6 g, 40 mmol), toluene (17.0 mL, 160 mmol), and $AlCl_3$ (5.33 g, 40 mmol), was stirred at room temperature for over 1.5 h. Then it was poured into amount of water. The system was extracted with ether and concentrated to recrystallize from ethanol to afford 6.70 g (68%) of product **1** as white pure powder. ^{1}H NMR (500 MHz, $CDCl_3$) δ 7.81 (d, J = 8.5 Hz, 4H, Ar), 7.28 (d, J = 8.5 Hz, 4H, Ar), 2.39 (s, 6H, CH_3).

Compound 2. A mixture of *p*-tolyl sulfone (10 g, 41 mmol) and *N*-bromosuccinimide (NBS) (22 g, 123 mmol) dissolved in 500 mL of benzene was refluxed in the presence of benzoyl peroxide (0.1 g, 0.41 mmol). After refluxing overnight, the reaction mixture was cooled and filtered. The transparent yellow filtrate was washed with distilled water and dried with anhydrous $MgSO_4$. The solvent was removed under reduced pressure to give a pale yellow solid, which was purified by flash column chromatography (petroleum ether : CH_2Cl_2 = 2 : 1) to afford 9.11 g (55%) of product **2** as a white solid. ^{1}H NMR (500 MHz, $CDCl_3$) δ 7.91 (d, J = 8.5 Hz, 4H, Ar), 7.53 (d, J = 8.5 Hz, 4H, Ar), 4.46 (s, 4H, CH_2).

Compound 3. A mixture of compound **2** (4.04 g, 10 mmol) and $P(OC_2H_5)_3$ (6.9 mL, 40 mmol) was refluxed for over 24 h under N_2. After distilling the liquid, the powder was recrystallized from *n*-hexane to give 3.27 g (63%) of product **3** as a white solid. ^{1}H NMR (500 MHz, $CDCl_3$) δ 7.87 (d, J = 8.5 Hz, 4H, Ar), 7.43 (d, J = 8.5 Hz, 4H, Ar), 4.01 (s, 8H, CH_2), 3.18 (d, 4H, CH_2), 1.22 (s, 12H, CH_3).

Compound G0–CHO. A mixture of TPA (10.0 g, 40 mmol) and $POCl_3$ (29.4 mL, 315 mmol) in DMF (30.0 mL, 388 mmol) was heated to 45 °C for 2.5 h, which was then poured into water and filtrated to obtained solid. The solid was purified through column chromatography using silica gel with chloroform as eluent to afford 10.0 g (90%) of **G0-CHO**. ^{1}H NMR (500 MHz, $CDCl_3$) δ 9.81 (s, 1H, CHO), 7.67 (d, J = 9.0 Hz, 2H, Ar), 7.34 (m, 4H, Ar), 7.17 (m, 6H, Ar), 7.01 (d, J = 8.5 Hz, 2H, Ar). MALDI-TOF MS: Calcd for $C_{19}H_{15}NO$ 273.1, Found: 273.6. Anal. Calcd for $C_{19}H_{15}NO$: C, 83.49; H, 5.53; N, 5.12%. Found: C, 83.90; H, 6.01; N, 5.07%.

Compound 4. 4-(*N*,*N*-Diphenylamino)benzaldehyde (14.00 g, 51.28 mmol), potassium iodide (11.43 g, 68.85 mmol) and acetic acid (210 mL) was heated to 85 °C and the solution was allowed to cool. Then the potassium iodate (10.97 g, 51.26 mmol) was added and the reaction was heated at 85 °C for 5 h. The solution was cooled to room temperature and poured into ice–water under stirring. The yellow precipitated solid was collected by filtration, and the collected solid was poured into 5% $NaHSO_3$ (100 ml) to eliminate I_2 and KIO_3. The final filtrated yellow solid was pure compound **4**. ^{1}H NMR (500 MHz, $CDCl_3$) δ 9.85 (s, 1H, CHO), 7.71 (d, J = 8.5 Hz, 2H, Ar), 7.63 (d, J = 8.5 Hz, 4H, Ar), 7.05 (d, J = 8.5 Hz, 2H, Ar), 6.89 (d, J = 8.5 Hz, 4H, Ar).

Compound 5. Methyltriphenylphosphonium bromide (4.28 g, 12 mmol) and **G0–CHO** (2.73 g, 10 mmol) were dissolved in 100 ml of dry THF, and the resulting solution was added dropwise slowly to *t*-BuOK (1.68 g, 15 mmol) in 30 ml of dry THF. The mixture was stirred for 8 h, and was then filtrated and evaporated to give the powder. The powder was purified using column chromatography (petroleum ether : CH_2Cl_2 = 4 : 1) to give 2.06 g (76%) of product **5** as a white solid. ^{1}H NMR (500 MHz, $CDCl_3$) δ 7.28 (d, J = 8.5 Hz, 2H, Ar), 7.23–7.26 (m, 4H, Ar), 7.09 (d, J = 8.0 Hz, 4H, Ar), 6.98–7.03 (m, 4H, Ar), 6.63–6.69 (m, 1H, CH), 6.63 (d, J = 16.5 Hz, 1H, CH=CH_2), 5.15 (d, J = 8.5 Hz, 1H, CH=CH_2).

Compound G1–CHO. Compound **4** (5.25 g, 10 mmol), compound **5** (7.0 g, 26 mmol) and K_3PO_4 (6.5 g, 30 mmol) were mixed in dimethylacetamide (DMAc) (50 mL) with 10 mg $Pd(OAc)_2$ as catalyst; the mixture was heated at 110 °C and stirred under an N_2 atmosphere for 24 h. After being cooled to room temperature, the reaction mixture was poured into water and extracted with CH_2Cl_2 (3 × 50 mL). The combined organic extracts were washed with brine, dried ($MgSO_4$), and concentrated to dryness under vacuum. The crude product was purified by flash column chromatography (petroleum ether : CH_2Cl_2 = 2 : 1) to give 4.47 g (55%) of product **G1–CHO** as a yellow solid. ^{1}H NMR (500 MHz, $CDCl_3$) δ 9.83 (s, 1H, CHO), 7.71 (d, J = 8.5 Hz, 2H, Ar), 7.45 (d, J = 8.5 Hz, 4H, Ar), 7.38 (d, J = 8.5 Hz, 4H, Ar), 7.25–7.28 (m, 12H, Ar), 7.10–7.15 (m, 12H, Ar), 7.00–7.06 (m, 8H, Ar), 6.96 (d, J = 16.5 Hz, 2H, Ar), MALDI-TOF MS: Calcd for $C_{59}H_{45}N_3O$ 812.0, Found: 812.9. Anal. Calcd for $C_{59}H_{45}N_3O$: C, 87.27; H, 5.59; N, 5.17%. Found: C, 87.15; H, 5.70; N, 5.09%.

Compound 6. G1–CHO (2.02 g, 2.5 mmol) and methyltriphenylphosphonium bromide (1.1 g, 3 mmol) were dissolved in 50 mL of dry THF. 0.45 mg (4 mmol) of *t*-BuOK in 10 mL of dry THF was added dropwise slowly to the resulting solution at 0 °C then the reaction mixture was warmed to room temperature and stirred under N_2 for 12 h. The reaction

mixture was poured into water and extracted with CH_2Cl_2 (3 × 50 mL). The combined organic extracts were washed with brine, dried ($MgSO_4$), and concentrated to dryness under vacuum. The crude product was purified by flash column chromatography (petroleum ether : CH_2Cl_2 = 4 : 1) to give 1.36 g (67%) of product **6** as a yellow solid. ^{1}H NMR (500 MHz, $CDCl_3$) δ 7.31–7.39 (m, 12H, Ar), 7.10–7.27 (m, 12H, Ar), 7.01–7.09 (m, 20H, Ar), 6.65–6.71 (m, 1H, CH), 6.70 (d, J = 17.5 Hz, 1H, CH═CH_2), 5.18 (d, J = 11.0 Hz, 1H, CH═CH_2), MALDI-TOF MS: Calcd for $C_{60}H_{47}N_3$ 809.4, Found: 811.4. Anal. Calcd for $C_{60}H_{47}N_3$: C, 88.96; H, 5.85; N, 5.19%. Found: C, 88.85; H, 6.01; N, 5.07%.

Compound G2–CHO. The synthesis of **G2–CHO** was similar to G1–CHO and characterized by ^{1}H NMR spectroscopy. ^{1}H NMR (500 MHz, $CDCl_3$) δ 9.83 (s, 1H, CHO), 7.71 (d, J = 8.5 Hz, 2H, Ar), 7.36–7.41 (m, 20H, Ar), 7.24–7.27 (m, 12H, Ar), 7.14 (d, J = 8.5 Hz, 2H, Ar), 7.08–7.12 (m, 30H, Ar), 6.96–7.05 (m, 32H, Ar). MALDI-TOF MS: calcd for $C_{139}H_{105}N_7O$ 1887.9, found: 1889.2. Anal. Calcd for $C_{139}H_{105}N_7O$: C, 88.36; H, 5.60; N, 5.19%. Found: C, 88.25; H, 5.73; N, 5.08%.

Compound G0. Compound **3** (155.6 mg, 0.3 mmol) and **G0–CHO** (213.2 mg, 0.78 mmol) were dissolved in 20 mL of dry THF and the resulting solution was added dropwise slowly to *t*-BuOK (107.7 mg, 0.96 mmol) in 10 mL of dry THF at 0 °C, then the reaction mixture was warmed to room temperature and stirred under N_2 overnight. The mixture was poured into water and extracted with dichloromethane. The organic phase was washed with water, brine and dried over $MgSO_4$. After removing the solvent, the product was purified by column chromatography using dichloromethane : petroleum ether (1 : 4) to give **G0** (177 mg, 78%) as a yellow solid. ^{1}H NMR (500 MHz, $CDCl_3$) δ 7.92 (d, J = 8.5 Hz, 4H), 7.78 (d, J = 8.5 Hz, 4H), 7.53 (d, J = 8.5 Hz, 4H), 7.40 (t, J = 8.0 Hz, 8H), 7.38 (d, J = 16 Hz, 2H), 7.18 (d, J = 16 Hz, 2H), 7.08 (t, J = 8.0 Hz, 4H), 7.05 (d, J = 8.5 Hz, 8H), 6.94 (d, J = 8.5 Hz, 4H). ^{13}C NMR (75 MHz $CDCl_3$) 148.266, 147.270, 142.599, 139.581, 131.814, 130.069, 129.340, 128.010, 129.790, 126.701, 124.814, 124.612, 123.408, 122.891. Anal. Calcd for $C_{52}H_{40}N_2O_2S$: C, 82.51; H, 5.33; N, 3.70%. Found: C, 82.62; H, 5.43; N, 3.62%.

Compound G1 and compound G2. The synthesis of **G1** and **G2** was similar to **G0** and the compounds were characterized from ^{1}H NMR and ^{13}C NMR spectra.

Compound **G1**: ^{1}H NMR (500 MHz, $CDCl_3$) δ 7.90 (d, J = 8.5 Hz, 4H), 7.58 (d, J = 8.5 Hz, 4H), 7.40 (d, J = 8.5 Hz, 10H), 7.37 (d, J = 8.5 Hz, 10H), 7.27 (d, J = 8.0 Hz, 4H), 7.25 (d, J = 7.5 Hz, 4H), 6.97–7.17 (m, 64 H). ^{13}C NMR (125 MHz, $CDCl_3$) 147.510, 146.083, 142.522, 139.586, 132.860, 131.766, 131.613, 130.558, 129.262, 129.023, 128.021, 127.883, 127.256, 127.182, 126.755, 126.271, 124.847, 124.615, 124.435, 123.971, 123.597, 123.455, 122.985, 122.480. MALDI-TOF MS: calcd for $C_{132}H_{100}N_6O_2S$ 1834.3, found: 1834.5. Anal. Calcd for $C_{132}H_{100}N_6O_2S$: C, 86.43; H, 5.49; N, 4.58%. Found: C, 86.31; H, 5.43; N, 4.62%.

Compound **G2**: ^{1}H NMR (500 MHz, $CDCl_3$) δ 7.90 (d, J = 8.0 Hz, 4H), 7.58 (d, J = 8.0 Hz, 4H), 7.36–7.41 (m, 52H, Ar), 7.24–7.27 (m, 28H, Ar), 6.96–7.17 (m, 140H, Ar). ^{13}C NMR (125 MHz, $CDCl_3$) 147.54, 147.11, 146.59, 146.373, 146.155, 142.532, 139.614, 132.809, 132.470, 132.144, 131.734, 130.894, 130.624, 130.072, 129.265, 129.016, 128.043, 127.904, 127.118, 127.031, 126.879, 126.773, 126.545, 126.402, 125.725, 124.893, 124.627, 124.422, 124.280, 124.177, 123.655, 123.525, 122.965. MALDI-TOF MS: falcd for $C_{292}H_{220}N_{14}O_2S$ 3989.0, found: 3990.2. Anal. Calcd for $C_{292}H_{220}N_{14}O_2S$: C, 87.92; H, 5.66; N, 4.92%. Found: C, 87.75; H, 5.78; N, 5.58%.

Acknowledgements

This work was supported by the State Key Development Program for Basic Research of China (Grant No.2009CB623605), the National Natural Science Foundation of China (Grant No. 50673035), Program for New Century Excellent Talents in Universities of China Ministry of Education, the 111 Project (Grant No. B06009), the Research Project of Jilin Province (Grant No.20080305) and the Graduated Innovation Fund of Jilin University (No.20080109).

Notes and references

1 H. Hoppe and N. S. Sariciftci, *J. Mater. Res.*, 2004, **19**, 1924.
2 C. Winder and N. S. Sariciftci, *J. Mater. Chem.*, 2004, **14**, 1077.
3 R. A. J. Janssen, J. C. Hummelen and N. S. Saricifti, *MRS Bull.*, 2005, **30**, 33.
4 K. M. Coakley and M. D. McGehee, *Chem. Mater.*, 2004, **16**, 4533.
5 H. Spanggaard and F. C. Krebs, *Sol. Energy Mater. Sol. Cells*, 2004, **83**, 125.
6 P. Peumans, A. Yakimov and S. R. Forrest, *J. Appl. Phys.*, 2003, **93**, 3693.
7 J. H. Hou, Z. A. Tan, Y. Yan, Y. J. He, C. H. Yang and Y. F. Li, *J. Am. Chem. Soc.*, 2006, **128**, 4911.
8 C. W. Tang, *Appl. Phys. Lett.*, 1986, **48**, 2.
9 J. B. Henk, G. S. Sonsoles and S. Sundarraj, *Chem. Commun.*, 2008, 618.
10 S. Roquet, A. Cravino, P. Leriche, O. Alévêque, P. Frère and J. Roncali, *J. Am. Chem. Soc.*, 2006, **128**, 3459.
11 (*a*) Y. Shirota, *J. Mater. Chem.*, 2000, **10**, 1; (*b*) Y. Shirota and H. Kageyama, *Chem. Rev.*, 2007, **107**, 953.
12 (*a*) J. Roncali, *Chem. Rev.*, 1997, **97**, 173; (*b*) P. Blanchard, P. Verlhac, L. Michaux, P. Frère and J. Roncali, *Chem.–Eur. J.*, 2006, **12**, 1244; (*c*) Roncali, *Chem. Soc. Rev.*, 2005, **34**, 483.
13 C. He, Q. G. He, X. D. Yang, G. L. Wu, C. Yang and F. L. Bai, *J. Phys. Chem. C*, 2007, **111**, 8661.
14 C. He, Q. G. He, Y. P. Yi, G. L. Wu, F. L. Bai, Z. G. Shuai and Y. F. Li, *J. Mater. Chem.*, 2008, **18**, 4085.
15 H. J. Xia, J. T. He, P. Peng, Y. H. Zhou, Y. W. Li and W. J. Tian, *Tetrahedron Lett.*, 2007, **48**, 5877.
16 G. N. Tew, M. U. Pralle and S. I. Stupp, *Angew. Chem., Int. Ed.*, 2000, **39**, 517.
17 P. Wei, X. Bi, Z. Wu and Z. Xu, *Org. Lett.*, 2005, **7**, 3199.
18 Z. Ning, Z. Chen, Q. Zhang, Y. Yan, S. Qian, Y. Cao and H. Tian, *Adv. Funct. Mater.*, 2007, **17**, 3799.
19 Q. Yao, E. P. Kinney and Z. Yang, *J. Org. Chem.*, 2003, **68**, 7528.
20 M. Lehmann, B. Schartel, M. Hennecke and H. Meier, *Tetrahedron*, 1999, **55**, 13377.
21 H. J. Xia, J. T. He, B. Xu, S. P. Wen, Y. W. Li and W. J. Tian, *Tetrahedron*, 2008, **64**, 5736.
22 Y. Jiang, J. Wang, Y. Ma, Y. Cui, Q. Zhou and J. Pei, *Org. Lett.*, 2006, **8**, 4287.
23 V. D. Mihailetchi, H. X. Xie, B. de Boer, L. J. A. Koster and P. W. M. Blom, *Adv. Funct. Mater.*, 2006, **16**, 699.

24 Y. H. Zhou, P. Peng, L. Han and W. J. Tian, *Synth. Met.*, 2007, **157**, 502.
25 Y. W. Li, L. L. Xue, H. J. Xia, S. P. Wen and W. J. Tian, *J. Polym. Sci., Part A: Polym. Chem.*, 2008, **46**, 3970.
26 X. M. Ma, J. L. Hua, W. J. Wu, Y. H. Jin, F. S. Meng, W. H. Zhan and H. Tian, *Tetrahedron*, 2008, **64**, 345.
27 M. J. Frisch, G. W. Trucks, H. B. Schlegel, G. E. Scuseria, M. A. Robb, J. R. Cheeseman, J. A. Montgomery, T. Vreven, Jr., K. N. Kudin, J. C. Burant, J. M. Millam, S. S. Iyengar, J. Tomasi, V. Barone, B. Mennucci, M. Cossi, G. Scalmani, N. Rega, G. A. Petersson, H. Nakatsuji, M. Hada, M. Ehara, K. Toyota, R. Fukuda, J. Hasegawa, M. Ishida, T. Nakajima, Y. Honda, O. Kitao, H. Nakai, M. Klene, X. Li, J. E. Knox, H. P. Hratchian, J. B. Cross, C. Adamo, J. Jaramillo, R. Gomperts, R. E. Stratmann, O. Yazyev, A. J. Austin, R. Cammi, C. Pomelli, J. W. Ochterski, P. Y. Ayala, K. Morokuma, G. A. Voth, P. Salvador, J. J. Dannenberg, V. G. Zakrzewski, S. Dapprich, A. D. Daniels, M. C. Strain, O. Farkas, D. K. Malick, A. D. Rabuck, K. Raghavachari, J. B. Foresman, J. V. Ortiz, Q. Cui, A. G. Baboul, S. Clifford, J. Cioslowski, B. B. Stefanov, G. Liu, A. Liashenko, P. Piskorz, I. Komaromi, R. L. Martin, D. J. Fox, T. Keith, M. A. Al-Laham, C. Y. Peng, A. Nanayakkara, M. Challacombe, P. M. W. Gill, B. Johnson, W. Chen, M. W. Wong, C. Gonzalez and J. A. Pople, *GAUSSIAN 03, Revision A.1*, Gaussian, Inc., Pittsburgh, PA, 2003.
28 A. P. Kulkarni, P. T. Wu, T. W. Kwon and S. A. Jenekhe, *J. Phys. Chem. B*, 2005, **109**, 19584.
29 Z. J. Ning, Q. Zhang, H. C. Pei, J. F. Luan, C. G. Lu and Y. C. H. Tian, *J. Phys. Chem. C*, 2009, **113**, 10307.
30 F. He, Y. H. Zhou, S. J. Liu, L. L. Tian, H. Xu, H. Y. Zhang, B. Yang, Q. Dong, W. Tian, Y. Ma and J. Shen, *Chem. Commun.*, 2008, 3912.